Cellular/Molecular

The Interface between Membrane-Spanning and Cytosolic Domains in Ca^{2+}-Dependent K^+ Channels Is Involved in β Subunit Modulation of Gating

Xiaohui Sun, Jingyi Shi, Kelli Delaloye, Xiao Yang, Huanghe Yang, Guohui Zhang, and Jianmin Cui

Department of Biomedical Engineering, Cardiac Bioelectricity and Arrhythmia Center, Center for the Investigation of Membrane Excitability Disorders, Washington University, St. Louis, Missouri 63130

Large-conductance, voltage-, and Ca^{2+}-dependent K^+ (BK) channels are broadly expressed in various tissues to modulate neuronal activity, smooth muscle contraction, and secretion. BK channel activation depends on the interactions among the voltage sensing domain (VSD), the cytosolic domain (CTD), and the pore gate domain (PGD) of the Slo1 α-subunit, and is further regulated by accessory β subunits (β1–β4). How β subunits fine-tune BK channel activation is critical to understand the tissue-specific functions of BK channels. Multiple sites in both Slo1 and the β subunits have been identified to contribute to the interaction between Slo1 and the β subunits. However, it is unclear whether and how the interdomain interactions among the VSD, CTD, and PGD are altered by the β subunits to affect channel activation. Here we show that human β1 and β2 subunits alter interactions between bound Mg^{2+} and gating charge R213 and disrupt the disulfide bond formation at the VSD–CTD interface of mouse Slo1, indicating that the β subunits alter the VSD–CTD interface. Reciprocally, mutations in the Slo1 that alter the VSD–CTD interaction can specifically change the effects of the β1 subunit on the Ca^{2+} activation and of the β2 subunit on the voltage activation. Together, our data suggest a novel mechanism by which the β subunits modulated BK channel activation such that a β subunit may interact with the VSD or the CTD and alter the VSD–CTD interface of the Slo1, which enables the β subunit to have effects broadly on both voltage and Ca^{2+}-dependent activation.

Introduction

Voltage- and Ca^{2+}-activated K^+ (BK) channels are composed of pore-forming α subunits encoded by the *slo1* gene and accessory β and γ subunits. Various β (β1–β4) or γ subunits modify channel properties differently (McManus et al., 1995; Xia et al., 1999; Brenner et al., 2000; Yan and Aldrich, 2010, 2012), providing a major mechanism for the diverse tissue-specific phenotypes. In brain, the β4 subunit is most abundant but other β subunits are also found (Brenner et al., 2000; Poulsen et al., 2009). The association of β4 subunits with Fragile X mental retardation protein modulates neurotransmission in hippocampal CA3 pyramidal neurons (Deng et al., 2013). A mutation of β3 is associated with human epilepsy (Lorenz et al., 2007). β Subunit function is fundamental for the molecular basis of BK channel-related physiological and pathophysiologic processes.

Received Feb. 10, 2013; revised May 21, 2013; accepted May 28, 2013.

Author contributions: X.S., H.Y., and J.C. designed research; X.S., J.S., K.D., X.Y., and G.Z. performed research; X.S. and G.Z. analyzed data; X.S., H.Y., and J.C. wrote the paper.

This work was supported by National Institutes of Health Grants R01-HL70393 and R01-NS060706 (to J.C.). J.C. is the Professor of Biomedical Engineering on the Spencer T. Olin Endowment. We thank Dr. Jimin Ding for helpful suggestions on the statistics of data analyses. The mSlo1 clone and hβ2 clone were kindly provided by Drs. Lawrence Salkoff and Chris Lingle (Washington University, St. Louis, MO) and by Dr. Robert Brenner (University of Texas Health Science Center at San Antonio, San Antonio, TX), respectively.

The authors declare no competing financial interests.

Correspondence should be addressed to Jianmin Cui, Department of Biomedical Engineering, Washington University in St. Louis, 290C Whitaker Hall, One Brookings Drive, St. Louis, MO 63130. E-mail: jcui@wustl.edu.

DOI:10.1523/JNEUROSCI.0620-13.2013

 0270-6474/13/3311253-09$15.00/0

The Slo1 subunit contains three structural domains: the cytosolic domain (CTD), which contains Ca^{2+} binding sites; the voltage sensing domain (VSD), which comprises the transmembrane segments S1–S4; and the pore gate domain (PGD), which comprises S5–S6 (Fig. 1). Interactions among these domains are important for the PGD to open in response to physiological stimulations of membrane potential, intracellular Ca^{2+} and Mg^{2+} (Lee and Cui, 2010). The β subunits share a similar membrane topology, with two transmembrane segments (TM1 and TM2), an extracellular loop, and the intracellular N-terminus and C-terminus. A BK channel contains four Slo1 subunits and up to four β subunits (Wang et al., 2002). TM1 and TM2 are packed at the mouth of the cleft between VSDs of two adjacent Slo1 subunits, with TM1 close to S1 of one VSD and TM2 close to S0 of adjacent VSD (Liu et al., 2010). The location of β subunits allows their interaction with the VSD, PGD, and CTD of Slo1, which may alter or constrain the interactions among these domains. However, such alteration and the consequence on BK channel activation have not been known or explored.

We began this study by investigating the effects of the β1 and β2 subunits on Mg^{2+}-dependent activation of BK channels. Previous studies showed that Mg^{2+} binds in between the VSD and CTD interface of Slo1 and interacts with gating charge R213 in S4 to activate the channel (Yang et al., 2007, 2008a; Fig. 1). In this study, we found that the β1 and β2 subunits reduce Mg^{2+} sensitivity and alter the Mg^{2+} binding site and the interaction between the bound Mg^{2+} with R213. Subsequently, we studied how mutations that change the VSD–CTD interface (Yang et al., 2013) affect the function of both β subunits. The results suggest that the

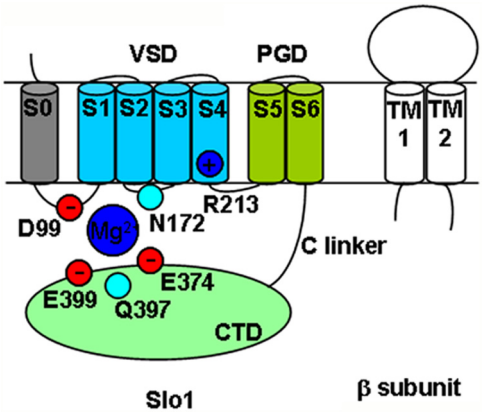

Figure 1. Membrane topology of BK channel α (Slo1; left) and β subunit (right). The Mg^{2+} binding sites (D99, N172, E374, and E399), Q397, C linker, and gating charge R213 are indicated.

association of β subunits alters the VSD–CTD interface and the VSD–CTD interface alteration in turn interferes with the action of both β subunits, providing a novel perspective on how β subunits modify BK channel activation.

Materials and Methods

Mutagenesis and expression. All point mutations were made from the *mbr5* splice variant of mouse Slo1 (mSlo1, GenBank accession number L16912; Butler et al., 1993) by using overlap-extension PCR (Shi et al., 2002) with *Pfu* polymerase (Stratagene). Human β1 and β2 (KCNMB1 and KCNMB2; GenBank accession numbers U25138 and AF209747) cDNAs were subcloned into pcDNA3.1(+). The β2 with N terminus-deleted (β2ND) subunit was created by removing amino acids from positions 2–20. The PCR-amplified regions for all constructs were verified by sequencing. cRNA was transcribed *in vitro* using T3 polymerase (Ambion) for all Slo1 constructs and T7 polymerase (Ambion) for β1 and β2ND subunits. We injected 0.05–50 ng of Slo1 cRNA or a mixture of 5–20 ng of Slo1 and 15–60 ng of β subunit cRNAs (the ratio of the amount of Slo1 to the amount of β is 1:3 to ensure the channel is saturated with β subunit) into *Xenopus laevis* oocytes (stage IV–V) 3–6 d before experiment (female *Xenopus laevis* were used here). Oocytes were incubated in ND96 solution (in mM: 96 NaCl, 2 KCl, 1.8 $CaCl_2$, 1 $MgCl_2$, 5 HEPES, pH 7.6) at 18°C.

Electrophysiology. Macroscopic and single-channel currents were recorded from excised inside-out patches formed with borosilicate pipettes of 0.6–1.0 MΩ resistance. Data were acquired by using an Axopatch 200-B patch-clamp amplifier (Molecular Devices) and Pulse acquisition software (HEKA Electronik). The current signals were low-pass filtered at 10 kHz with the four-pole Bessel filter built in the amplifier and digitized at 20 μs intervals. For most of the macroscopic current recordings, capacity and leak currents were subtracted using a P/5 protocol with a holding potential of −120 mV. However, with currents recorded in the presence of either β1 or β2ND at 100 μM $[Ca^{2+}]$, no leak subtraction was conducted. The pipette solution contained the following (in mM): 140 potassium methanesulfonic acid ($KMeSO_3$), 20 HEPES, 2 KCl, and 2 $MgCl_2$, pH 7.2. The basal internal solution contained the following (in mM): 140 $KMeSO_3$, 20 HEPES, 2 KCl, 1 EGTA, 22 mg/l 18-crown-6-tetracarboylic acid (Sigma-Aldrich), pH 7.2. $CaCl_2$ standard solution was added to obtain the desired free $[Ca^{2+}]$, which was measured by a Ca^{2+}-sensitive electrode (Thermo Electron). The nominal 0 μM $[Ca^{2+}]$ solution contained 5 mM EGTA with no added Ca^{2+}, and the free $[Ca^{2+}]$ is calculated to be ~0.5 nM. The 2-(trimethylammonium)ethyl methanethiosulfonate bromide (MTSET) and dithiothreitol (DTT) working solutions were diluted from the stock to the final concentration of 0.2 and 10 mM, respectively, by using the nominal 0 μM $[Ca^{2+}]$ solution. The MTSET solution was freshly prepared right before each perfusion since its lifetime is ~10 min. DTT, MTSET, or DTT-plus-MTSET treatments were performed by perfusing excised patch with 10 mM DTT for 5 min, with 200 μM MTSET for 3 min, or with 10 mM DTT for 5 min before 3 min 200 μM MTSET perfusion, respectively.

Gating currents were recorded in the inside-out configuration as well. The pipette solution contained the following (in mM): 127 tetraethylammonium (TEA), 125 $HMeSO_3$, 2 HCl, 2 $MgCl_2$, and 20 HEPES, pH 7.2. The internal solution contains (in mM) the following: 141 *N*-ethyl-D-glucamine, 135 $HMeSO_3$, 6 HCl, 20 HEPES, and 5 EGTA, pH 7.2. To prevent the saturation of fast capacitive transients, voltage commands were filtered at 20 kHz with an eight-pole Bessel filter (Frequency Devices; Horrigan and Aldrich, 1999). Data were sampled at 100 kHz with an 18-bit analog-to-digital converter (ITC-18, Instrutech) and filtered at 10 kHz with an internal filter of Axopatch (Molecular Devices). Capacitive transients and leak currents were subtracted using a P/5 protocol with a holding potential of −120 mV. All experiments were conducted at room temperature (22–24°C).

Data analyses. Relative conductance was determined by measuring tail current amplitudes at negative voltages as indicated for the wild-type (WT) and mutant Slo1 channels with and without β subunits. The gating charge movements were determined by integrating the area under the rising phase and single exponential fits to the decaying phase of on gating current at various voltages. The *G–V* relationship or the charge–voltage (*Q–V*) relations of the WT and mutant channels with and without β subunits were fitted with the Boltzmann equation as follows in Equation 1:

$$\frac{G}{G_{\max}} = \frac{1}{1 + \exp\left(-\frac{zF(V - V_{1/2})}{RT}\right)}$$

or in Equation 2:

$$\frac{Q}{Q_{\max}} = \frac{1}{1 + \exp\left(-\frac{zF(V - V_{1/2})}{RT}\right)}$$

In Equation 1, $G/G_{\max}$ is the ratio of conductance to maximum conductance, z is the number of equivalent charges, V is membrane potential, $V_{1/2}$ is the voltage at which the channel is 50% activated, F is the faraday constant, R is gas constant, and T is the absolute temperature. In Equation 2, Q/Q_{max} is the ratio of gating charge to maximum gating charge, z is the gating charge associated with voltage sensor movement, $V_{1/2}$ is the voltage for half of the gating charge movements at the closed conformation of the channel, and the other parameters have the same meaning as in Equation 1. Free energy change (ΔG) were calculated as $\Delta(z * V_{1/2})$ (Cui and Aldrich, 2000). Mg^{2+} sensitivity refers to 10 mM Mg^{2+}-induced *G–V* relationship shift. Ca^{2+} sensitivity refers to 100 μM Ca^{2+}-induced *G–V* relationship shift.

For limiting slope measurement, the open probability of single channels was analyzed with Igor Pro software (WaveMetrics) and plotted at relative membrane potentials to construct a P_O–V relation, which was then fitted to the HCA (Horrigan, Cui, and Aldrich) model as the following Equation 3 (Horrigan et al., 1999):

$$P_o = \frac{1}{1 + \frac{\exp\left(-\frac{z_L FV}{RT}\right)}{L_o}\left(\frac{1 + \exp\left(\frac{z_J F(V - V_{hc})}{RT}\right)}{1 + \exp\left(\frac{z_J F(V - V_{ho})}{RT}\right)}\right)^4}$$

where z_L is the charge associated with gate opening when all the voltage sensors are at their resting state; z_J is the charge associated with voltage sensor movements; L_0 is the intrinsic open probability at 0 mV while all the voltage sensors are at their resting state; and V_{hc} and V_{ho} are the voltages for half of the voltage sensors to be at their activation state at the closed and the open conformations of the gate, respectively.

Curve fittings were performed using the Levenberg–Marquardt algorithm in Igor Pro software (WaveMetrics) for nonlinear least-squares fits. The means of the data were obtained by averaging from 3

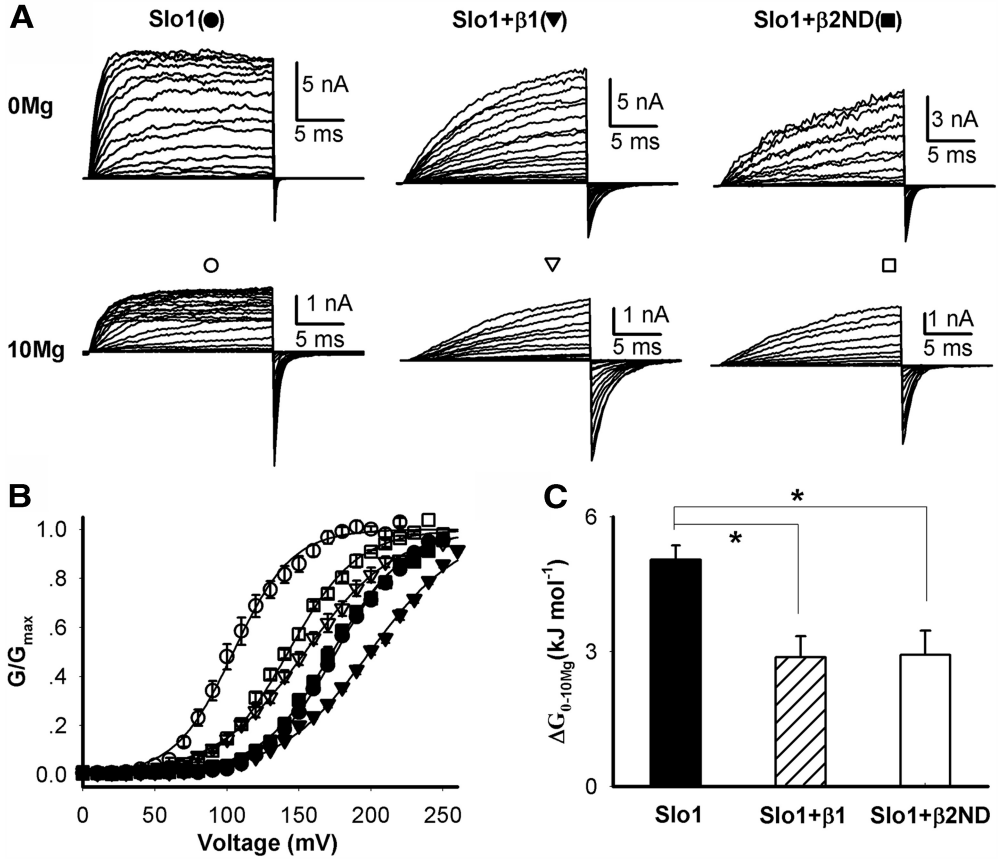

Figure 2. Effects of β subunits on Mg^{2+} sensitivity of BK channel activation. ***A***, Macroscopic current traces of Slo1, Slo1-plus-β1 (Slo1 + β1), and Slo1-plus-β2ND (Slo1 + β2ND) channels from inside-out patches in 0 (top) and 10 mM [Mg^{2+}] (bottom). The [Ca^{2+}] is 0. Currents were elicited by voltages ranging from 0 to 250 mV for 20 ms with 10 mV increments at 0 [Mg^{2+}], or from −100 to 250 mV at 10 mM [Mg^{2+}]. The prepulse potential was −80 mV for 20 ms (only the last 0.5 ms shown), and the repolarization potential was −80 mV. ***B***, Normalized *G–V* relations of Slo1, Slo1 + β1, and Slo1 + β2ND in 0 and 10 mM [Mg^{2+}], indicated by symbols shown in ***A***. Solid lines are fits to the Boltzmann equation (Materials and Methods, Eq. 1). ***C***, Free energy change induced by [Mg^{2+}] changes from 0 to 10 mM ($\Delta G_{0\text{--}10\ Mg}$). The Mg^{2+}-dependent free energy change associated with channel gating ($\Delta G_{0\text{--}10\ Mg}$) was calculated as $z * V_{1/2\ 0\ Mg} - z * V_{1/2\ 10\ Mg}$, where *z* is the valence of the apparent gating charge obtained from the Boltzmann fitting of the *G–V* relation and $V_{1/2}$ is the voltage at half maximum *G–V* (Cui and Aldrich, 2000). The number of patches (*n*) for each channel in 0 and 10 mM [Mg^{2+}] is as follows: Slo1, $n = 9, 4$; Slo1 + β1, $n = 16, 9$; Slo1 + β2ND, $n = 6, 7$, respectively. Two-way ANOVA was used to test the differences of $\Delta G_{0\text{--}10\ Mg}$ between channels: $^*p = 0.013$, Slo1 + β1 versus Slo1; $p = 0.006$, Slo1 + β2ND versus Slo1.

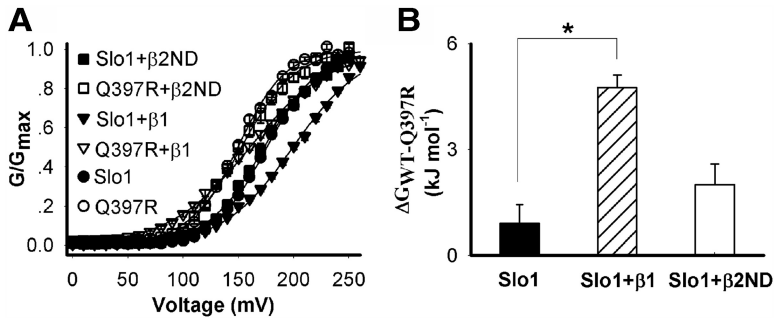

Figure 3. Effects of β subunits on R213–R397 interaction. ***A***, Normalized *G–V* relations of WT and Q397R with or without β1 or β2ND from inside-out patches at 0 [Ca^{2+}]. Solid lines are fittings to the Boltzmann equation. ***B***, Differences of free energy between WT and Q397R channels ($\Delta G_{WT\text{-}Q397R}$). For Slo1, Q397R, Slo1 plus β1 (Slo1 + β1), Q397R plus β1 (Q397R + β1), Slo plus β2ND (Slo1 + β2ND), and Q397R plus β2ND (Q397R + β2ND), $n = 9, 5, 16, 14, 6, 7$, respectively. Two-way ANOVA was used to test the differences of $\Delta G_{WT\text{-}Q397R}$ with and without β subunits: $^*p < 0.0001$, Slo1 + β1 versus Slo1; $p = 0.082$, Slo1 + β2ND versus Slo1.

to 16 patches and error bars represent SEM. Statistics were performed using GraphPad Prism5 software (GraphPad Software) and SPSS software (IBM). Unpaired Student's *t* test and multiple ANOVA were performed and a *p*-value of <0.05 is considered significant.

Results

β1 and β2ND subunits reduce Mg^{2+} sensitivity of BK channel activation

Both β1 and β2ND (β2 N terminus-deleted mutation to eliminate β2-induced inactivation; see Materials and Methods) subunits enhance Ca^{2+} sensitivity of BK channels (McManus et al., 1995; Nimigean and Magleby, 1999; Wallner et al., 1999; Xia et al., 1999; Orio and Latorre, 2005; Lee et al., 2010). We studied whether β1 and β2ND subunits also affect Mg^{2+} sensitivity of the channel. As shown in Figure 2, coexpression of β1 or β2ND significantly reduced the Mg^{2+} sensitivity of the BK channel. In contrast to a 64.4 ± 3.3 mV leftward shift of the *G–V* curve in the absence of β subunits, 10 mM Mg^{2+} induced only 34.3 ± 2.4 and 37.2 ± 1.5 mV leftward shift in the presence of β1 and β2ND, respectively (Fig. 2*B*). When converted to free energy changes (ΔG) 10 mM Mg^{2+} induced 5.0 ± 0.3, 2.9 ± 0.5, and 2.9 ± 0.5 kJ/mol of free energy changes for Slo1 alone, Slo1 plus β1, and Slo1 plus β2ND, respectively (Fig. 2*C*).

Next, we investigated the underlying mechanism of reduced Mg^{2+} sensitivity induced by the β subunits. Previous studies showed that Mg^{2+} binds at VSD–CTD interface of Slo1 channels with two coordinate residues (D99 and N172) from VSD and another two (E374 and E399) from CTD (Fig. 1; Shi et al., 2002; Xia et al., 2002; Yang et al., 2008a). The bound Mg^{2+} interacts with gating charge R213 (Fig. 1) to activate the channel (Hu et al., 2003; Yang et al., 2007, 2008a). Disturbance of either the distance or relative orientation between the bound Mg^{2+} and R213 or Mg^{2+} binding site could alter the response of BK channels to Mg^{2+} stimulation. We first examined whether the former mechanism contributed to a reduction in Mg^{2+} sensitivity. To avoid the complication of possible changes in Mg^{2+} binding, we measured the changes of the interaction between R213 and Q397R in response to the association of the β subunits (Fig. 3). Our previous study showed that positively charged residue 397R can mimic Mg^{2+} to interact with gating charge R213 (Yang et al., 2007) and shift *G–V* relationship of BK channels to the left (Fig. 3*A*). The change of R213–R397 electrostatic interaction, therefore, could be used to probe the relative distance or direction changes between these two residues. As shown in Figure 3*A*, in the presence of β1, the difference of $V_{1/2}$ between WT and 397R mutant channels increased compared with the channels comprising Slo1 alone (36.6 ± 2.8 mV for Slo1 plus β1; 23.1 ± 2.6 mV for Slo1 alone), whereas the 397R-induced *G–V* shift reduced in the presence of β2ND (17.5 ± 4.6 mV). Correspondingly, β1 increased free energy difference between WT and Q397 mutant channels significantly (4.8 ± 0.3 kJ/mol vs 0.9 ± 0.5 kJ/mol, Slo1 plus β1 vs Slo1 alone; Fig. 3*B*). Although β2ND reduced *G–V* shift, it increased the steepness of the *G–V* slope. Therefore, β2ND also increased free energy difference between WT and Q397 mutant channels (2.0 ± 0.6 kJ/mol Slo1 plus β2ND; Fig. 3*B*). These results indicate that the presence of β1 and perhaps β2ND as well alters distance, orientation, or both between residue 213 and 397.

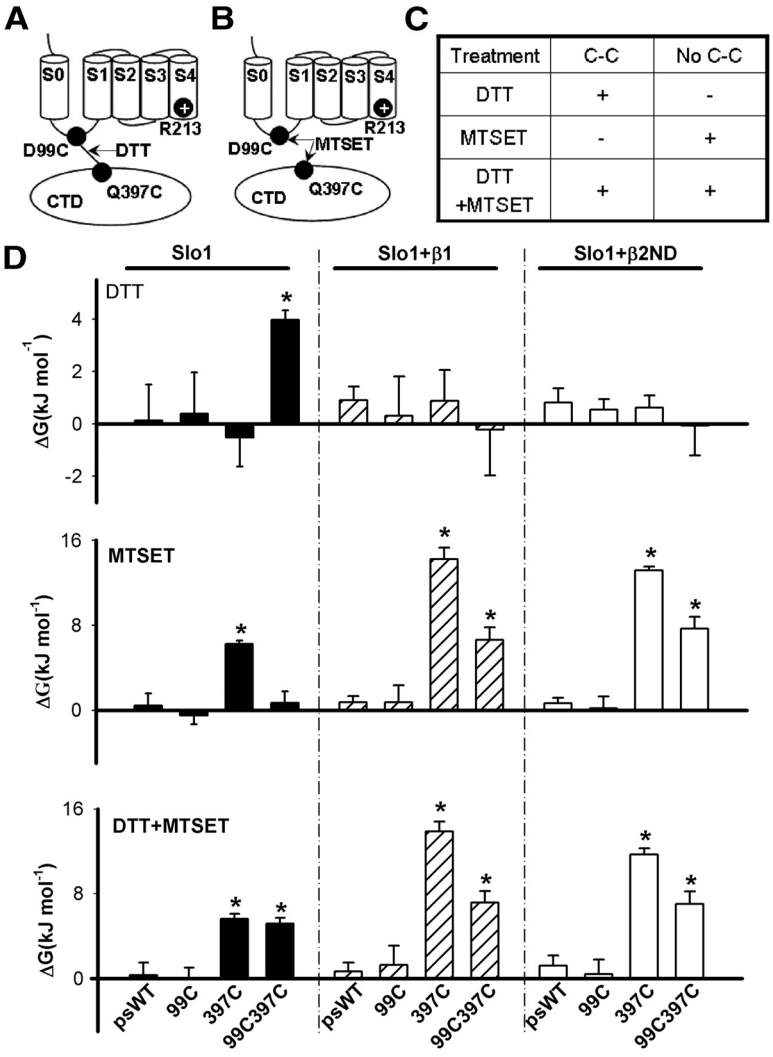

Figure 4. Effects of β subunits on disulfide bond formation between C99 and C397. ***A***, ***B***, Diagrams show the disulfide bond formed (***A***) and not formed (***B***) between D99C and Q397C. ***C***, The expected responses of channels to different chemical treatments with (C-C) or without (No C-C) the C99 –C397 disulfide bond formation. DTT, 10 mM DTT treatment for 5 min; MTSET, 200 μM MTSET treatment for 3 min; DTT-plus-MTSET (DTT + MTSET), 10 mM DTT for 5 min followed with a 200 μM MTSET treatment for 3 min. +, response in the form of a shift in *G–V* relations; −, no response. ***D***, Free energy differences (Δ*G*) before and after DTT (top), MTSET (middle), or DTT + MTSET (bottom) treatment in the presence of no β (black columns), β1 (hatched columns), or β2ND (white columns) at 0 [Ca^{2+}]. psWT, pseudo-wild-type Slo1 with C430 mutated to A, while all mutations, D99C, Q397C and D99CQ397C, were made in the background of C430A. For psWT, D99C, Q397C, D99CQ397C, psWT plus β1 (psWT + β1), D99C plus β1 (D99C + β1), Q397C plus β1 (Q397C + β1), D99CQ397C plus β1 (D99CQ397C + β1), psWT plus β2ND (psWT + β2ND), D99C plus β2ND (D99C + β2ND), Q397C plus β2ND (Q397C + β2ND), and D99CQ397C plus β2ND (D99CQ397C + β2ND), $n = 5, 4, 3, 5, 3, 3, 3, 6, 4, 4, 5, 4$ before DTT, and $n = 4, 3, 5, 3, 4, 3, 5, 4, 5, 4, 5, 5$ after DTT; $n = 5, 4, 3, 5, 3, 3, 3, 6, 4, 4, 5, 4$ before MTSET, and $n = 3, 3, 4, 4, 4, 4, 5, 5, 4, 3, 4, 4$ after MTSET; $n = 5, 4, 3, 5, 3, 3, 3, 6, 4, 4, 5, 4$ before DTT + MTSET, and $n = 4, 3, 5, 3, 4, 4, 7, 7, 3, 3, 9, 5$ after DTT + MTSET, respectively. Unpaired *t* tests were used to compare *G* before and after indicated treatments: $^*p < 0.0001$.

β1 and β2ND subunits disrupt disulfide bond formation between C99 and C397

Residue 213 and 397 are located in the membrane-spanning VSD and the CTD, respectively (Fig. 1). It is unlikely that the association of β1 and β2ND subunit with Slo1 would change the distance or orientation between just these two residues. The results in Figure 3 thus suggest that the interface between the VSD and CTD, which includes residues 213 and 397, is changed by the β1 and β2ND subunit. To examine this hypothesis, we investigated whether another pair of residues, D99 and Q397 in the membrane-spanning and cytosolic domains, respectively (Fig. 1), also changes distance or orientation. Our previous study showed that C99 and C397, which resulted from mutations D99C and Q397C, could spontaneously form a disulfide bond in BK channels comprising Slo1 alone (Yang et al., 2008a). The disulfide bond formation requires certain distance (2.9–4.6 Å) and appropriate orientation between two cysteines (Hazes and Dijkstra, 1988). If C99 and C397 no longer form disulfide bond in the presence of β subunits, it suggests that the distance or orientation between the two residues is changed, thus supporting a change in the interfacial confirmation by β subunits.

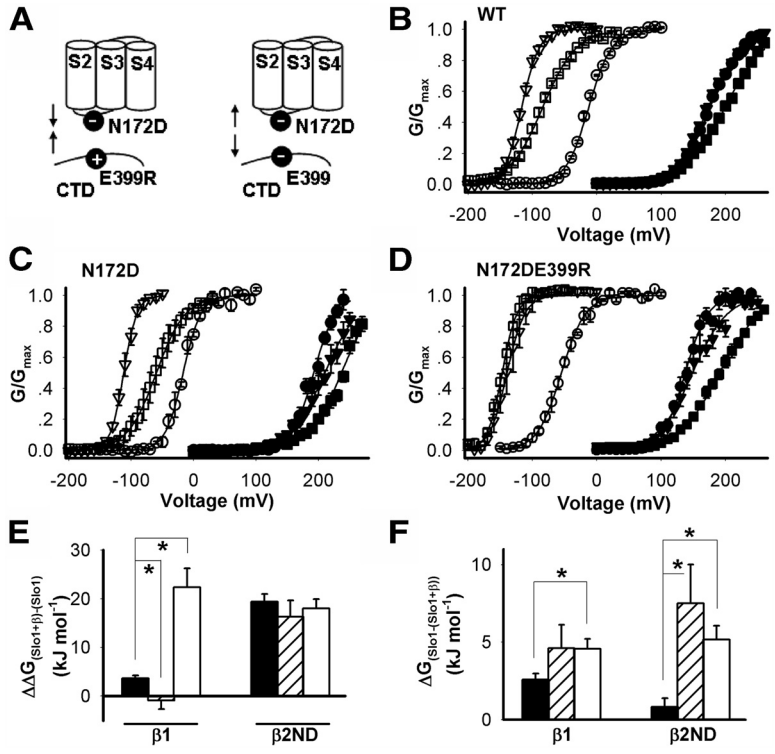

Figure 5. Mutation-induced changes in the VSD–CTD interface alter β subunit modulation of Ca^{2+} and voltage-dependent activation. ***A***, Diagrams show attraction (left, N172DE399R) and repulsion (right, N172DE399) electrostatic interactions between 172 (in the VSD) and 399 (in the CTD). ***B–D***, Normalized *G–V* relations of WT (***B***), N172D (***C***), and N172DE399R (***D***) Slo1 in the presence of no β (circles), β1 (squares), or β2ND (triangles) at 0 (closed symbols) or 100 μM [Ca^{2+}] (open symbols). Solid lines are fittings to the Boltzmann equation. ***E***, Differences in Ca^{2+}-dependent free energy changes (Δ*G* measured between 0 and 100 μM [Ca^{2+}]) with and without β subunits ($\Delta\Delta G_{(Slo1+\beta)-(Slo1)}$) for the WT (black), N172D (hatched), and N172DE399R (white) channels, respectively. ***F***, Free energy difference with and without β subunits at 0 [Ca^{2+}] ($\Delta G_{(Slo1-(Slo1+\beta))}$) for the WT (black), N172D (hatched), and N172DE399R (white) channels, respectively. The number of patches (*n*) for 0 and 100 μM [Ca^{2+}] is as follows: WT Slo1, $n = 9, 6$; WT Slo plus β1 (Slo1+β1), $n = 16, 4$; WT Slo1 plus β2ND (Slo1+β2ND), $n = 6, 4$; N172D Slo1, $n = 6, 3$; N172D Slo1+β1, $n = 3, 3$; N172D Slo1+β2ND, $n = 6, 3$; N172DE399R Slo1, $n = 4, 3$; N172DE399R Slo1+β1, $n = 6, 3$; N172DE399R Slo1+β2ND, $n = 4, 6$. Three-way ANOVA was used to test $\Delta\Delta G_{(Slo1+\beta)-(Slo1)}$ in ***E*** between WT and mutant channels. *$p = 0.01$, N172D plus β1 (N172D+β1) versus WT plus β1 (WT+β1); $p < 0.0001$, N172DE399R plus β1 (N172DE399R+β1) versus WT+β1. Two-way ANOVA was used to test $\Delta G_{(Slo1-(Slo1+\beta))}$ in ***F*** between WT and mutant channels. *$p = 0.011$, N172DE399R+β1 versus WT+β1; $p = 0.008$, N172D+β2ND versus WT+β2ND; $p < 0.0001$, N172DE399R+β2ND versus WT+β2ND.

DTT and MTSET reagents were used to detect the formation of the disulfide bond. DTT is a reducing agent that can break disulfide bond into single cysteines (Fig. 4*A*), whereas MTSET can covalently modify single cysteines and introduce a positive charge into cysteine (Fig. 4*B*). C430A was used as pseudo-WT (psWT) here since C430 in native Slo1 channel can be modified by MTSET and affect channel activation (Zhang and Horrigan, 2005). Our previous studies showed that if C99 and C397 form a disulfide bond, DTT treatment affects channel activation and shifts the *G–V* curve to the left, whereas MTSET has no effect on channel gating since the disulfide bond protects C99 and C397 from MTSET modification; however, if treating channels with DTT first to break the disulfide bond, both C397 and C99 will be available for MTSET modification and the modification of C397 shifts *G–V* relation to more negative voltages (Yang et al., 2008a). On the other hand, if C99 and C397 does not form disulfide bond, DTT should not affect channel gating, whereas MTSET would modify channel activation with or without DTT pretreatment (Fig. 4*C*).

We repeated the previous experiments on channels comprising Slo1 alone and obtained results as expected for a disulfide bond being formed between C99 and C397 (Fig. 4*C*,*D*, left, black columns). DTT treatment (Fig. 4*D*, top left) shifted *G–V* relation to left, corresponding to a free energy change of 4.0 ± 0.4 kJ/mol, only in the double mutation D99CQ397C (disulfide bond formed) but not in three control channels, psWT, D99C, or Q397C (no disulfide bond formed). On the other hand, MTSET treatment (Fig. 4*D*, middle left) shifted *G–V* to more negative voltages, corresponding to a free energy change of 6.2 ± 0.3 kJ/mol in only Q397C, but not in D99CQ397C. After the pretreatment of DTT, however, MTSET treatment (Fig. 4*D*, bottom left) shifted *G–V* of both Q397C and D99CQ397C to more negative voltages.

Contrast to the results on channels comprising Slo1 alone (Fig. 4*D*, left, black columns), the results on channels with the coexpression of β1 (Fig. 4*D*, middle, hatched columns) or β2ND (Fig. 4*D*, right, white columns) are consistent with no disulfide bond being formed between C99 and C397 (Fig. 4*C*). DTT treatment had no effect on D99CQ397C or any of the control channels (Fig. 4*D*, top middle and right), while MTSET treatment shifted G–*V* of both Q397C and D99CQ397C to more negative voltages, corresponding to significant free energy changes (Fig. 4*D*, middle middle and right). Pretreatment of DTT did not affect the results of MTSET treatment (Fig. 4*D*, bottom middle and right). These results indicate that the association of the β1 and β2ND subunits disrupted the formation of the disulfide bond between C99 and C397, supporting the idea that the β subunits altered the VSD–CTD interface. Considering that D99 is one of the Mg^{2+} binding residues and the Mg^{2+} binding site is formed between the VSD–CTD domains, these results suggest that Mg^{2+} binding could be perturbed by β subunits.

A VSD–CTD interface change alters the function of both β1 and β2ND subunits

If the association of the β1 and β2ND subunits alters the Slo1 VSD–CTD interfacial confirmation, a perturbation of the interfacial conformation might reciprocally alter the function of the β subunits. Recently we found that artificially introduced charged residues at residues 172 and 399 in the Mg^{2+} binding site could alter VSD–CTD interfacial confirmation and affect voltage- and Ca^{2+}-dependent activation of BK channels through electrostatic interaction (Yang et al., 2013). To examine whether the β subunit modulation of BK channel was altered, we used N172D, a mutation that causes repulsion between the VSD and CTD (Fig. 5*A*, right), or N172DE399R, a mutation that causes attraction between the VSD and CTD (Fig. 5*A*, left).

Figure 5 shows the effects of N172D and N172DE399R on *G–V* relations in 0 and 100 μM [Ca^{2+}] of channels with and without the β subunits. For channels comprising Slo1 alone, the Ca^{2+} sensitivity, as

measured by *G–V* shift ($\Delta V_{1/2\ 0-100\ Ca}$) due to [$Ca^{2+}$] increase from 0 to 100 μM, was increased by repulsion mutation N172D (213.3 ± 1.6 mV vs 189.7 ± 3.7 mV; N172D vs WT) but was reduced slightly by attraction mutation N172DE399R (187.5 ± 1.2 mV; Fig. 5*B–D*). To examine whether the mutations alter the effects of β subunits on Ca^{2+} sensitivity, Figure 5*E* plots the change of Ca^{2+}-sensitive free energy caused by β subunits ($\Delta\Delta G_{((Slo1+\beta)-Slo1)}$) in WT (black), N172D (hatched), and N172DE399R (white), where ΔG_{Slo1} and $\Delta G_{(Slo1\ +\ \beta)}$ is the free energy change due to [Ca^{2+}] increase from 0 to 100 μM ($\Delta G_{0\text{-}100\ Ca}$) for the channels comprising Slo1 only and Slo1 plus β subunit, respectively. In the presence of β1, N172D significantly reduced the difference of Ca^{2+} sensitivity between Slo1-plus-β1 and Slo1 channels, whereas N172DE399R significantly enhanced this difference compared with WT channels (Fig. 5*C–E*), indicating that the VSD–CTD interface change alters the effects of β1 on Ca^{2+} sensitivity of Slo1 channels. However, both mutations failed to alter the effect of Slo1 plus β2ND on Ca^{2+} sensitivity (Fig. 5*C–E*), suggesting that the VSD–CTD interface change caused by 172–399 interactions had no effect on β2ND modulation of Ca^{2+} sensitivity.

On the other hand, the VSD–CTD interface change caused by 172–399 interactions altered the effects of both β subunits on voltage dependence of the channel, For the WT channel, the association of the β1 subunit shifted the *G–V* relation at 0 [Ca^{2+}] to more positive voltages, whereas the association of the β2ND subunit caused no such shift (Fig. 5*B*). These results are consistent with previous reports and are considered evidence that the β1 subunit alters voltage dependence of BK channels (Cox and Aldrich, 2000; Orio and Latorre, 2005; Wang and Brenner, 2006). With the mutation N172D (Fig. 5*C*) and N172DE399R (Fig. 5*D*), the *G–V* at 0 [Ca^{2+}] was shifted more to right by the β1 subunit (*G–V* shifted 23.2 ± 2.0 mV, 43.6 ± 4.3 mV, and 52.7 ± 6.4 mV for the WT, N172D, and N172DE399R, respectively). It's more striking that the *G–V* at 0 [Ca^{2+}] was shifted to right by the β2ND subunit with the mutation N172D (Fig. 5*C*) and N172DE399R (Fig. 5*D*) as well, given that β2ND does not shift the *G–V* relation for WT channel (*G–V* shifted −2.4 ± 1.9 mV, 19.6 ± 5.8 mV, and 9.2 ± 8.7 mV for the WT, N172D, and N172DE399R, respectively). Figure 5*F* plots the free energy differences between channels comprising Slo1 alone and channels with β subunits at 0 [Ca^{2+}] ($\Delta G_{[Slo1\ -\ (Slo1\ +\ \beta)]}$) in WT (black), N172D (hatched), and N172DE399R (white). In the presence of β1, WT channels show 2.6 ± 0.4 kJ/mol free energy change and both N172D and N172DE399R increase free energy change by ~1.1 kJ/mol. However, the *G–V* relation of WT Slo1-plus-β2ND channels shifts a little compared with those of WT Slo1 channels (0.8 ± 0.6 kJ/mol). Both mutations caused 6–9-fold higher free energy differences between channels with and without β2ND subunits, indicating a significant alteration of β2ND modulation of voltage dependence by the mutation-induced VSD–CTD interface changes.

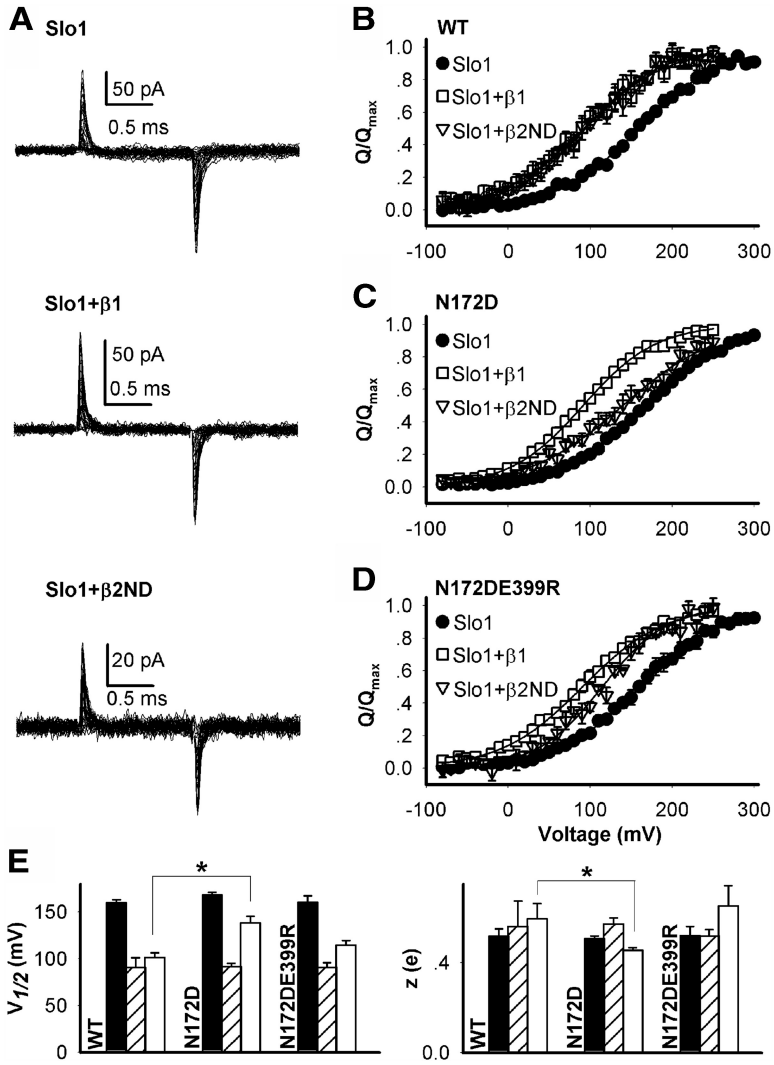

Figure 6. Mutation-induced changes in the VSD–CTD interface alter β subunit modulation of voltage sensor movements. ***A***, Representative gating current recordings of WT Slo1 with and without β subunits. The prepulse potential was −80 mV for 20 ms (shown only the last 0.5 ms), and the repolarization potential was −80 mV. ***B–D***, Normalized *Q–V* curves of WT (***B***), N172D (***C***), and N172DE399R (***D***) in the presence of no β (closed circles), β1 (open square), or β2ND (open triangles). Currents were elicited by voltage pulses of −80 to +300 mV for 1 ms with 10 mV increments. ***E***, $V_{1/2}$ (left) and *z* (right) of the *Q–V* curves of WT and mutant channels in the presence of no β (black), β1 (hatched) and β2ND (white). WT Slo1, $n = 7$; WT Slo1 plus β1 (Slo1 + β1), $n = 6$; WT Slo1 plus β2ND (Slo1 + β2ND), $n = 6$; N172D Slo1, $n = 5$; N172D Slo1 + β1, $n = 3$; N172D Slo1 + β2ND, $n = 5$; N172DE399R Slo1, $n = 4$; N172DE399R Slo1 + β1, $n = 5$; N172DE399R Slo1 + β2ND, $n = 3$. Unpaired *t* tests were used to test the difference between mutant and WT channels. For $V_{1/2}$ on the left: $^*p = 0.0015$, N172D plus β2ND (N172D + β2ND) versus WT plus β2ND (WT + β2ND); for *z* on the right: $p = 0.041$, N172D + β2ND versus WT + β2ND.

The above results suggest that modulation of voltage dependence by β2ND is more significantly altered than by β1 when the VSD–CTD interface is changed by mutations N172D and N172DE399R. This result was further confirmed by gating current measurements (Fig. 6). Similar with previous studies (Bao and Cox, 2005; Contreras et al., 2012), the presence of β1 shifts the *Q–V* relation leftward by 69.1 ± 10.7 mV (Fig. 6*B*). However, neither N172D nor N172DE399R affects *Q–V* relationship with or without β1 (Fig. 6*B–E*), suggesting that the mutation-induced VSD–CTD interface change does not affect β1 modulation of the

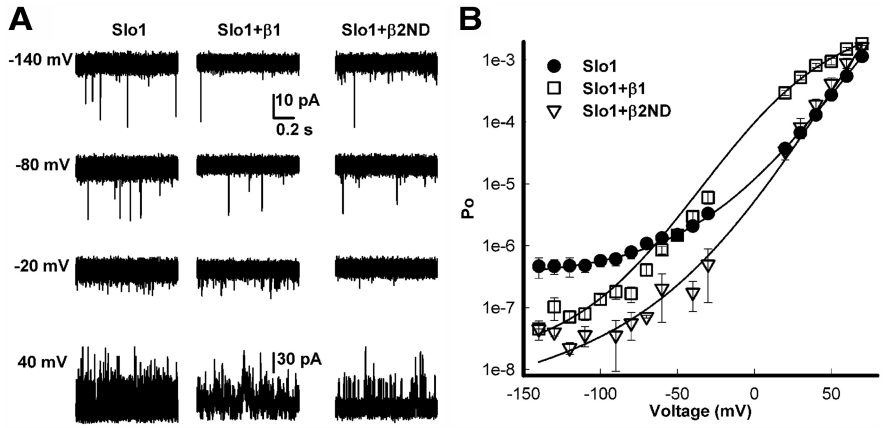

Figure 7. Effects of β subunits on the intrinsic open probability of BK channel activation gate. ***A***, Current traces of unitary openings from Slo1, Slo1 plus β1 (Slo1+β1), and Slo1 plus β2ND (Slo1+β2ND) channels elicited by indicated voltages from inside-out patches expressing hundreds of channels at 0 [Ca^{2+}]. All the traces share the same current and time scales except for the current trace of Slo1+β1 at 40 mV (the current scale is labeled just above this trace). ***B***, Averaged P_0–V relations for Slo1 (closed circles, $n = 7$), Slo1+β1 (open squares, $n = 8$), and Slo1+β2ND (open triangles, $n = 3$) channels at 0 [Ca^{2+}]. Solid lines are fittings to the HCA model (see Materials and Methods) with fixed parameters $z_L = 0.1, z_J = 0.59$ for Slo1; $z_L = 0.1, z_J = 0.69$ for Slo1+β1; and $z_L = 0.3, z_J = 0.59$ for Slo1+β2ND, while L_0, V_{hc}, and V_{ho} are optimized for the best fitting. $L_0 = 3.5 \times 10^{-7}$ for Slo1; 3.6×10^{-8} for Slo1+β1, and 4.9×10^{-8} for Slo1+β2ND. V_{hc} and V_{ho} values are as follows: Slo1, 160 and −16.9 mV; Slo1+β1, 16.6 and −88.8 mV; Slo1+β2ND, 160 and −35.8 mV.

voltage sensor. To the contrary, in the presence of β2ND the Q–V relation was shifted by the mutations. $V_{1/2}$ of the Q–V relation was 101.4 ± 4.9 mV, 138.5 ± 6.9 mV, and 114.8 ± 4.7 mV when β2ND was associated with WT (Fig. 6*B*), N172D (Fig. 6*C*), and N172DE399R Slo1 (Fig. 6*D*), respectively. Figure 6*E* plots $V_{1/2}$ and z value of Q–V curves of the channels without (black bars) and with the coexpression of the β1 (hatched bars) or β2ND subunit (white bars) for the WT and mutant channels. Together, the results in Figure 5 and 6 show that the VSD–CTD interface change alters the effects of β subunits on Ca^{2+} and voltage-dependent gating. Interestingly, β1 function and β2ND function were altered differently: the VSD–CTD interface change altered β1 modulation of Ca^{2+} sensitivity more significantly than β1 modulation of voltage-dependent gating; meanwhile, VSD–CTD interface change altered β2ND modulation of voltage dependent gating more significantly than β2ND modulation of Ca^{2+} sensitivity.

β1 and β2ND subunits reduce intrinsic open probability of the pore

In addition to affecting the functions of VSD and CTD of BK channels, β subunits also alter the intrinsic properties of the PGD (Fig. 7). Previous studies showed that the pore of BK channels can open with a small open probability in the absence of Ca^{2+} and without voltage sensor activation at negative voltages (<−80 mV) (Horrigan et al., 1999). This intrinsic P_o reflects the properties of the PGD and its interaction with other structure domains (VSD and CTD). The intrinsic P_o of BK channels is obtained by recording the unitary currents in a patch that contains hundreds of channels at negative voltages (<−20 mV; Horrigan et al., 1999; Cui and Aldrich, 2000; Fig. 7*A*). The results show that both β1 and β2ND reduced intrinsic P_o, which is consistent with previous study (Orio and Latorre, 2005), indicating that the intrinsic pore gate property is altered by both β subunits. Thus, the β subunits not only alter the interface between VSD and CTD, but also affect conformation in the PGD.

Discussion

In this study, we find that both β1 and β2ND reduce Mg^{2+} sensitivity of BK channel activation possibly by altering the VSD–CTD interfacial conformation (Figs. 2, 3). Since Mg^{2+} binding site is formed by the residues from both the VSD and CTD (Yang et al., 2008a), the Mg^{2+} coordinating residues in the two structural domains engage in electrostatic interactions (Yang et al., 2013) that may help stabilize the conformation of the binding site, and the bound Mg^{2+} activates BK channels by interacting with a positive charge in the S4 voltage sensor (Yang et al., 2007; Fig. 1). The reduced Mg^{2+} sensitivity by β subunits therefore led to our discovery that the association of β subunits alters the interface between the VSD and CTD and thus the interactions between the two structural domains across the interface. This mechanism is supported by two additional lines of evidence: the association of β1 and β2ND subunits disrupts a disulfide bond formation between the VSD and CTD (Fig. 4) and, conversely, the disturbance of the VSD–CTD interface by mutations also alters the function of the β subunits (Figs. 5, 6).

A change in the VSD–CTD interface conformation and interactions by the association of β subunits is consistent with the functional and structural characteristics of β subunit modulation of BK channel function. Functionally, β subunits cause broad changes in BK channel gating properties. For example, the β1 and β2 subunits alter voltage-dependent activation by shifting the voltage dependence of gating charge movements (Bao and Cox, 2005; Savalli et al., 2007; Contreras et al., 2012), enhance Ca^{2+} sensitivity (McManus et al., 1995; Nimigean and Magleby, 1999; Wallner et al., 1999; Xia et al., 1999; Brenner et al., 2000), and reduce the intrinsic open probability of the channel in the absence of Ca^{2+} binding and voltage sensor activation (Orio and Latorre, 2005; Wang and Brenner, 2006). Corresponding to this functional diversity, multiple structural sites are involved in direct or allosteric interactions between Slo1 and β subunits. The sites of β subunits implicated in such interactions include the extracellular loop (Hanner et al., 1998; Meera et al., 2000; Zeng et al., 2003; Lv et al., 2008; Gruslova et al., 2012), the membrane spanning segments (Morera et al., 2012), and the intracellular termini (Orio et al., 2006; Wang and Brenner, 2006), while the sites in Slo1 include extracellular N terminus (Morrow et al., 2006), transmembrane segment S0 (Wallner et al., 1996; Morrow et al., 2006; Lee et al., 2010), and the N terminus of the cytosolic RCK1 domain (Lee et al., 2010). The multisite interactions between Slo1 and β subunits would likely alter the VSD–CTD interface and the interactions among CTD, PGD, and VSD that are the key in voltage- and Ca^{2+}-dependent activation of BK channels (Niu et al., 2004; Lee and Cui, 2010; Yuan et al., 2010, 2012; Horrigan, 2012; Yang et al., 2013; Zhang et al., 2013).

In addition to demonstrating a change of VSD–CTD interface during BK channel gating, our results also suggest that the VSD–CTD interface change plays an active role in β subunit modulation. We found that perturbations of the VSD–CTD interface by

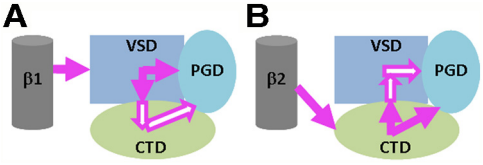

Figure 8. The VSD–CTD interface mediated allosteric pathways for β1 (***A***) and β2 (***B***) subunit regulation of BK channel gating. β1, β1 subunit; β2, β2 subunit; solid arrows, direct interactions between β subunits and Slo1; hollow arrows, indirect interactions propagated via the VSD–CTD interface. It is not known whether the β subunits directly interact with PGD so that the interaction between β subunits and PGD is not depicted here for simplicity.

mutations N172D and N172DE399R alter the ability of the β1 subunit to modify Ca^{2+} sensitivity more sharply than those same perturbations alter the ability of the β2ND to modify Ca^{2+} sensitivity (Fig. 5). Meanwhile, and conversely, those perturbations alter the ability of β2ND to modify voltage dependence more significantly than they alter the ability of β1 to modify voltage dependence (Figs. 5, 6). This differential influence can be explained by the mechanism that the β1 subunit primarily interacts with the VSD to alter voltage-dependent gating (Yang et al., 2008b), while such an interaction changes the VSD–CTD interface to alter Ca^{2+}-dependent gating (Fig. 8*A*, hollow arrows); on the other hand, the β2ND subunit primarily interacts with the CTD to alter Ca^{2+}-dependent gating (Lee et al., 2010), while such an interaction changes the VSD–CTD interface to alter voltage-dependent gating (Fig. 8*B*, hollow arrows). Thus the VSD–CTD interface changes provide an allosteric mechanism to propagate the effects of different β subunits to all aspects of BK channel gating, and the perturbation of the VSD–CTD interface has a lesser influence on the effects of the primary interaction between a β subunit and Sol1 than on the downstream allosteric effects.

The proposed mechanism (Fig. 8) may also explain many previous, sometimes puzzling, observations. A number of laboratories, by fitting allosteric models to experimental data, showed that β1 increases apparent Ca^{2+} sensitivity of BK channels mainly through the changes of VSD activation and the intrinsic probability of PGD rather than through the changes in Ca^{2+} binding or its coupling to the activation gate (Cox and Aldrich, 2000; Orio and Latorre, 2005; Wang and Brenner, 2006). Mutagenesis and chimera experiments also showed that neither the Ca^{2+} bowl nor the AC (βA∼αC) region that contains the other Ca^{2+} binding site influenced β1-enhanced Ca^{2+} sensitivity (Qian et al., 2002; Lee et al., 2010). Furthermore, mutations in the Slo1 VSD that alter VSD activation (Ma et al., 2006) have been shown to eliminate or reduce the effect of the β1 subunit on Ca^{2+} sensitivity (Yang et al., 2008b). These results suggest that the β1 subunit increases Ca^{2+} sensitivity of BK channels by altering VSD activation. On the other hand, the macroscopic current recordings showed that the β2 subunit has little effect on either $V_{1/2}$ or slope of the *G–V* relationship of Slo1 at 0 Ca^{2+} (Fig. 5*B*; Orio and Latorre, 2005; Lee et al., 2010). Consistently, mutagenesis experiments identified the cytosolic AC (βA∼αC) region as important for β2 to increase Ca^{2+} sensitivity, but mutations in VSD had only small effects on that (Yang et al., 2008b; Lee et al., 2010). These results all suggest that the β2 subunit targets the cytosolic domain but not the VSD to modulate BK channel sensitivity to Ca^{2+}. Nevertheless, voltage-clamp fluorometry and gating current measurements showed that the β2 subunit alters voltage sensor activation (Fig. 6; Savalli et al., 2007; Contreras et al., 2012). These results are consistent with our proposed mechanism (Fig. 8).

In this study, the changes in the VSD–CTD interface by β subunit association was probed by changes in Mg^{2+} sensitivity (Fig. 2), interactions between R397 and R213 (Fig. 3), and disulfide bond formation between C99 and C397 (Fig. 4). These specific interactions were changed to different degrees in the presence of the β1 or β2ND subunit, indicating that the two β subunits may alter the VSD–CTD interface differently. The interactions between the VSD and CTD have just begun to be investigated and it is clear from the results of Figure 7 that β subunits also affect PGD properties, which might be through the VSD–CTD interface as well or through a direct interaction with PGD. So far only a few specific interactions among the three structural domains important for Ca^{2+}- and voltage-dependent activation have been identified (Niu et al., 2004; Lee and Cui, 2010; Yuan et al., 2010, 2012; Horrigan, 2012; Yang et al., 2013; Zhang et al., 2013). How β subunits affect these interactions to alter Ca^{2+}- and voltage-dependent activation of BK channels remains to be elucidated in future studies.

References

Bao L, Cox DH (2005) Gating and ionic currents reveal how the BKCa channel's Ca^{2+} sensitivity is enhanced by its beta1 subunit. J Gen Physiol 126:393–412. CrossRef Medline

Brenner R, Jegla TJ, Wickenden A, Liu Y, Aldrich RW (2000) Cloning and functional characterization of novel large conductance calcium-activated potassium channel beta subunits, hKCNMB3 and hKCNMB4. J Biol Chem 275:6453–6461. CrossRef Medline

Butler A, Tsunoda S, McCobb DP, Wei A, Salkoff L (1993) mSlo, a complex mouse gene encoding "maxi" calcium-activated potassium channels. Science 261:221–224. CrossRef Medline

Contreras GF, Neely A, Alvarez O, Gonzalez C, Latorre R (2012) Modulation of BK channel voltage gating by different auxiliary beta subunits. Proc Natl Acad Sci U S A 109:18991–18996. CrossRef Medline

Cox DH, Aldrich RW (2000) Role of the beta1 subunit in large-conductance Ca(2+)-activated K(+) channel gating energetics. Mechanisms of enhanced Ca(2+) sensitivity. J Gen Physiol 116:411–432. CrossRef Medline

Cui J, Aldrich RW (2000) Allosteric linkage between voltage and Ca(2+)-dependent activation of BK-type mslo1 K(+) channels. Biochemistry 39:15612–15619. CrossRef Medline

Deng PY, Rotman Z, Blundon JA, Cho Y, Cui J, Cavalli V, Zakharenko SS, Klyachko VA (2013) FMRP regulates neurotransmitter release and synaptic information transmission by modulating action potential duration via BK channels. Neuron 77:696–711. CrossRef Medline

Gruslova A, Semenov I, Wang B (2012) An extracellular domain of the accessory β1 subunit is required for modulating BK channel voltage sensor and gate. J Gen Physiol 139:57–67. CrossRef Medline

Hanner M, Vianna-Jorge R, Kamassah A, Schmalhofer WA, Knaus HG, Kaczorowski GJ, Garcia ML (1998) The beta subunit of the high conductance calcium-activated potassium channel. Identification of residues involved in charybdotoxin binding. J Biol Chem 273:16289–16296. CrossRef Medline

Hazes B, Dijkstra BW (1988) Model building of disulfide bonds in proteins with known three-dimensional structure. Protein Eng 2:119–125. Medline

Horrigan FT (2012) Perspectives on: conformational coupling in ion channels: conformational coupling in BK potassium channels. J Gen Physiol 140:625–634. CrossRef Medline

Horrigan FT, Aldrich RW (1999) Allosteric voltage gating of potassium channels II. Mslo channel gating charge movement in the absence of Ca(2+). J Gen Physiol 114:305–336. CrossRef Medline

Horrigan FT, Cui J, Aldrich RW (1999) Allosteric voltage gating of potassium channels I. Mslo ionic currents in the absence of Ca(2+). J Gen Physiol 114:277–304. CrossRef Medline

Hu L, Shi J, Ma Z, Krishnamoorthy G, Sieling F, Zhang G, Horrigan FT, Cui J (2003) Participation of the S4 voltage sensor in the Mg2+-dependent activation of large conductance (BK) K+ channels. Proc Natl Acad Sci U S A 100:10488–10493. CrossRef Medline

Lee US, Cui J (2010) BK channel activation: structural and functional insights. Trends Neurosci 33:415–423. CrossRef Medline

Lee US, Shi J, Cui J (2010) Modulation of BK channel gating by the β2

subunit involves both membrane-spanning and cytoplasmic domains of Slo1. J Neurosci 30:16170–16179. CrossRef Medline

Liu G, Niu X, Wu RS, Chudasama N, Yao Y, Jin X, Weinberg R, Zakharov SI, Motoike H, Marx SO, Karlin A (2010) Location of modulatory beta subunits in BK potassium channels. J Gen Physiol 135:449–459. CrossRef Medline

Lorenz S, Heils A, Kasper JM, Sander T (2007) Allelic association of a truncation mutation of the KCNMB3 gene with idiopathic generalized epilepsy. Am J Med Genet B Neuropsychiatr Genet 144B:10–13. CrossRef Medline

Lv C, Chen M, Gan G, Wang L, Xu T, Ding J (2008) Four-turn alpha-helical segment prevents surface expression of the auxiliary hbeta2 subunit of BK-type channel. J Biol Chem 283:2709–2715. Medline

Ma Z, Lou XJ, Horrigan FT (2006) Role of charged residues in the S1–S4 voltage sensor of BK channels. J Gen Physiol 127:309–328. CrossRef Medline

McManus OB, Helms LM, Pallanck L, Ganetzky B, Swanson R, Leonard RJ (1995) Functional role of the beta subunit of high conductance calcium-activated potassium channels. Neuron 14:645–650. CrossRef Medline

Meera P, Wallner M, Toro L (2000) A neuronal beta subunit (KCNMB4) makes the large conductance, voltage- and Ca2+-activated K+ channel resistant to charybdotoxin and iberiotoxin. Proc Natl Acad Sci U S A 97:5562–5567. CrossRef Medline

Morera FJ, Alioua A, Kundu P, Salazar M, Gonzalez C, Martinez AD, Stefani E, Toro L, Latorre R (2012) The first transmembrane domain (TM1) of beta2-subunit binds to the transmembrane domain S1 of alpha-subunit in BK potassium channels. FEBS Lett 586:2287–2293. CrossRef Medline

Morrow JP, Zakharov SI, Liu G, Yang L, Sok AJ, Marx SO (2006) Defining the BK channel domains required for beta1-subunit modulation. Proc Natl Acad Sci U S A 103:5096–5101. CrossRef Medline

Nimigean CM, Magleby KL (1999) The beta subunit increases the Ca2+ sensitivity of large conductance Ca2+-activated potassium channels by retaining the gating in the bursting states. J Gen Physiol 113:425–440. CrossRef Medline

Niu X, Qian X, Magleby KL (2004) Linker-gating ring complex as passive spring and Ca(2+)-dependent machine for a voltage- and Ca(2+)-activated potassium channel. Neuron 42:745–756. CrossRef Medline

Orio P, Latorre R (2005) Differential effects of beta 1 and beta 2 subunits on BK channel activity. J Gen Physiol 125:395–411. CrossRef Medline

Orio P, Torres Y, Rojas P, Carvacho I, Garcia ML, Toro L, Valverde MA, Latorre R (2006) Structural determinants for functional coupling between the beta and alpha subunits in the Ca2+-activated K+ (BK) channel. J Gen Physiol 127:191–204. CrossRef Medline

Poulsen AN, Wulf H, Hay-Schmidt A, Jansen-Olesen I, Olesen J, Klaerke DA (2009) Differential expression of BK channel isoforms and beta-subunits in rat neuro-vascular tissues. Biochim Biophys Acta 1788:380–389. CrossRef Medline

Qian X, Nimigean CM, Niu X, Moss BL, Magleby KL (2002) Slo1 tail domains, but not the Ca2+ bowl, are required for the beta 1 subunit to increase the apparent Ca2+ sensitivity of BK channels. J Gen Physiol 120:829–843. CrossRef Medline

Savalli N, Kondratiev A, de Quintana SB, Toro L, Olcese R (2007) Modes of operation of the BKCa channel beta2 subunit. J Gen Physiol 130:117–131. CrossRef Medline

Shi J, Krishnamoorthy G, Yang Y, Hu L, Chaturvedi N, Harilal D, Qin J, Cui J (2002) Mechanism of magnesium activation of calcium-activated potassium channels. Nature 418:876–880. CrossRef Medline

Wallner M, Meera P, Toro L (1996) Determinant for beta-subunit regulation in high-conductance voltage-activated and Ca(2+)-sensitive K+ channels: an additional transmembrane region at the N terminus. Proc Natl Acad Sci U S A 93:14922–14927. CrossRef Medline

Wallner M, Meera P, Toro L (1999) Molecular basis of fast inactivation in voltage and Ca2+-activated K+ channels: a transmembrane beta-subunit homolog. Proc Natl Acad Sci U S A 96:4137–4142. CrossRef Medline

Wang B, Brenner R (2006) An S6 mutation in BK channels reveals beta1 subunit effects on intrinsic and voltage-dependent gating. J Gen Physiol 128:731–744. CrossRef Medline

Wang YW, Ding JP, Xia XM, Lingle CJ (2002) Consequences of the stoichiometry of Slo1 α and auxiliary β subunits on functional properties of large-conductance Ca^{2+}-activated K+ channels. J Neurosci 22:1550–1561. Medline

Xia XM, Ding JP, Lingle CJ (1999) Molecular basis for the inactivation of Ca^{2+}- and voltage-dependent BK channels in adrenal chromaffin cells and rat insulinoma tumor cells. J Neurosci 19:5255–5264. Medline

Xia XM, Zeng X, Lingle CJ (2002) Multiple regulatory sites in large-conductance calcium-activated potassium channels. Nature 418:880–884. CrossRef Medline

Yan J, Aldrich RW (2010) LRRC26 auxiliary protein allows BK channel activation at resting voltage without calcium. Nature 466:513–516. CrossRef Medline

Yan J, Aldrich RW (2012) BK potassium channel modulation by leucine-rich repeat-containing proteins. Proc Natl Acad Sci U S A 109:7917–7922. CrossRef Medline

Yang H, Hu L, Shi J, Delaloye K, Horrigan FT, Cui J (2007) Mg2+ mediates interaction between the voltage sensor and cytosolic domain to activate BK channels. Proc Natl Acad Sci U S A 104:18270–18275. CrossRef Medline

Yang H, Shi J, Zhang G, Yang J, Delaloye K, Cui J (2008a) Activation of Slo1 BK channels by Mg2+ coordinated between the voltage sensor and RCK1 domains. Nat Struct Mol Biol 15:1152–1159. CrossRef Medline

Yang H, Zhang G, Shi J, Lee US, Delaloye K, Cui J (2008b) Subunit-specific effect of the voltage sensor domain on Ca2+ sensitivity of BK channels. Biophys J 94:4678–4687. CrossRef Medline

Yang J, Yang H, Sun X, Delaloye K, Yang X, Moller A, Shi J, Cui J (2013) Interaction between residues in the Mg2+-binding site regulates BK channel activation. J General Physiology 141:217–228. CrossRef Medline

Yuan P, Leonetti MD, Pico AR, Hsiung Y, MacKinnon R (2010) Structure of the human BK channel Ca2+-activation apparatus at 3.0 A resolution. Science 329:182–186. CrossRef Medline

Yuan P, Leonetti MD, Hsiung Y, MacKinnon R (2012) Open structure of the Ca2+ gating ring in the high-conductance Ca2+-activated K+ channel. Nature 481:94–97. CrossRef Medline

Zeng XH, Xia XM, Lingle CJ (2003) Redox-sensitive extracellular gates formed by auxiliary beta subunits of calcium-activated potassium channels. Nat Struct Biol 10:448–454. CrossRef Medline

Zhang G, Horrigan FT (2005) Cysteine modification alters voltage- and Ca(2+)-dependent gating of large conductance (BK) potassium channels. J Gen Physiol 125:213–236. CrossRef Medline

Zhang GH, Yang JQ, Yang HH, Shi JY, Yang X, Delaloye K, Moller A, Cui J (2013) Electrostatic interaction between the S4–S5 linker and the cytoplasmic end of S6 regulates BK channel gating. Philadelphia: Biophysics Society 57th Annual Meeting, 2367-Pos.